Available online at www.sciencedirect.com
ScienceDirect
Surface Science 600 (2006) 3285–3296
SURFACE SCIENCE
www.elsevier.com/locate/susc

Competition between associative and dissociative adsorption of 1,2-dihalogenated benzenes on Si(1 0 0)2 × 1: Formation of dihalocyclohexadiene, halophenyl and phenylene adstructures

X.J. Zhou, K.T. Leung *

Department of Chemistry, University of Waterloo, Waterloo, Ont., Canada N2L 3G1

Received 11 February 2006; accepted for publication 16 June 2006
Available online 12 July 2006

Abstract

The room temperature (RT) adsorption of 1,2-difluorobenzene (1,2-DFB), 1,2-dichlorobenzene (1,2-DCB) and 1,2-dibromobenzene (1,2-DBB) on Si(1 0 0)2 × 1 have been investigated by X-ray photoelectron spectroscopy (XPS) and temperature programmed desorption (TPD). Both XPS and TPD data show that the relative degree of dissociative to associative adsorption of the dihalogenated benzene (DXB) appears to increase with decreasing electronegativity of the halogen atom (X). In particular, the C 1s intensity ratios for the C–H and C–Si components to the C–X component are found to be 2, 3 and 9.6 for 1,2-DFB, 1,2-DCB and 1,2-DBB, respectively. These results indicate that 1,2-DFB, like benzene, exclusively adsorbs molecularly as a difluorocyclohexadiene adspecies on Si(1 0 0)2 × 1 while 1,2-DBB adsorbs predominantly with double debromination to form 1,2-phenylene. The majority of 1,2-DCB (75%) is found to adsorb molecularly, with the rest (25%) undergone single or double dechlorination to form chlorophenyl and phenylene, respectively. All three DXB molecules appear to have similar coverage as benzene. The two molecular desorption features for 1,2-DFB and 1,2-DCE are observed with desorption maxima at 460 K and 540 K similar to those found for benzene, which suggests that the dihalocyclohexadiene adstructures involve similar bonding through the benzene ring. In accord with the XPS data, no molecular desorption feature is observed for 1,2-DBB on the 2 × 1 surface. Further decomposition of the resulting phenylene adstructures is evident from the desorption fragment, C_2H_2, found at 610 K and 740 K. Recombinative desorption of HCl and HBr above 880 K are also found for 1,2-DCB and 1,2-DBB, respectively. The observed differences between associative and dissociative adsorption for the three DXB adsorbates could be attributed not only to the large difference in the C–X bond strength but also to the relative contributions from inductively withdrawing and resonantly donating electrons exerted by the halogen (X) atoms to the benzene ring.

Keywords: Dihalobenzene; Dihalocyclohexadiene; Halophenyl; Phenylene; Si(1 0 0)2 × 1; Dissociative and associative chemisorption; X-ray photoelectron spectroscopy; Temperature programmed desorption

1. Introduction

Continual miniaturization of silicon devices requires better fundamental understanding of silicon surface chemistry, particularly the mechanisms driving selective reactions and functionalization as well as self-organization of the reactants and products on the surface. The Si(1 0 0)2 × 1 surface provides an excellent substrate for modification by organic molecules to develop two-dimensional molecular templates for nanoscale and molecular electronic applications [1]. Organic molecules can be used to facilitate and manipulate molecular self-arrangement upon adsorption by careful choice of the attaching functional groups with the appropriate steric effects and lateral interactions. Among the wide variety of organic molecules, unsaturated hydrocarbons with one or more double bonds (e.g., ethylene [2,3], butadienes [4], and benzene [5,6]) are particularly interesting, because they provide π electrons to interact

* Corresponding author.
E-mail address: tong@uwaterloo.ca (K.T. Leung).

0039-6028/$ - see front matter © 2006 Elsevier B.V. All rights reserved.
doi:10.1016/j.susc.2006.06.023

with the Si dangling bonds on the 2×1 surface in a typical cycloaddition reaction. On the other hand, molecules with lone-pair electrons could adsorb molecularly by forming dative bonding (e.g., pyridine [7]) and/or dissociatively (e.g., aliphatic amines [8], and pyrrole [9]). Studies of the interactions of these molecules with the 2×1 surface could therefore provide important insights into organosilicon surface chemistry and help to develop potential applications in emerging technologies.

As the simplest alkene and the most common aromatic hydrocarbon, respectively, ethylene and benzene have been extensively investigated by using a variety of techniques [2,3,8,7]. In particular, ethylene is known to adsorb on Si(1 0 0)2×1 by forming two Si–C covalent bonds in a [2+2] cycloaddition configuration. In the case of chlorinated and brominated ethylenes, our recent work showed that abstraction of the halogen atom (X) occurs with the C═C bond remaining intact upon adsorption [10–12]. To account for these observations, we proposed a new insertion adsorption mechanism, in which the Si atom is in effect inserted into the C–X bond by cleavage of the Si–Si σ bond and the formation of Si–X and Si–C bonds [11]. Unlike ethylene, benzene is found to adsorb on the 2×1 surface with multiple configurations, including a predominant di-σ bonded [2 + 4] cycloaddition adstructure, and tetra-σ bonded "tight bridge" and "twist bridge" adstructures as the minor configurations [13,14]. Furthermore, methyl-substituted benzenes, such as toluene (with single methyl substitution) [15,16] and xylene (with double methyl substitution) [17,18], appear to undergo stronger reactions with the 2×1 surface, particularly H abstraction from the methyl groups, in addition to the cycloaddition reaction observed for the benzene ring. On the other hand, styrene (with vinyl or ethenyl substitution) [19–22] and phenylacetylene or ethynylbenzene (with ethynyl substitution) [23] could only react with Si(1 0 0)2×1 through the vinyl and ethynyl group, respectively. Hydrogen replacement by different organic functional groups (methyl, vinyl and ethynyl) on the benzene ring could therefore produce remarkably different surface chemistry on the 2×1 surface. Compared to methyl, vinyl and ethynyl substituted benzenes, halogen-substituted benzenes are expected to follow different surface chemistries. In particular, Naumkin et al. investigated chlorinated benzenes on Si(1 0 0)2×1 by using scanning tunnelling microscopy (STM) and ab initio quantum calculations [24,25]. Their work showed that, in addition to adsorption through the benzene ring as similarly found for benzene on the 2×1 surface at room temperature (RT), chlorinated benzenes also exhibit dissociative adsorption with C–Cl bond breakage but with the benzene ring intact [24,25]. This result is in marked contrast to the result found for Si(1 1 1)7×7 on which no C–Cl dissociation was found at RT [26,27], unless photon-induced [26] or STM-based electron induced C–Cl dissociation [27] were employed.

In the present work, we focus on the effects of double substitution of different halogen atoms (F, Cl, and Br) on the mechanism of benzene adsorption on Si(1 0 0)2×1 at RT, particularly the competition between associative (cycloaddition) and dissociative (dehalogenation) adsorption. The halogen atom could either donate its valence electrons to the benzene ring through the p orbitals by resonance or withdraw the π electrons from the benzene ring through induction [28]. Depending on the relative degree of electron donation or withdrawal, the halogen atom could either enhance or reduce the reactivity of the benzene ring. The differences in the electron densities or electronegativities of the different halogen atoms (F, Cl, and Br) could therefore lead to different reaction pathways for these halogenated benzenes. Furthermore, the large variations in the bond strengths among the C–F (132 kcal/mol), C–Cl (95 kcal/mol), and C–Br bond (67 kcal/mol) and with respect to those of the C–H (81 kcal/mol) and C–C (83 kcal/mol) [and C═C bond (146 kcal/mol)] [29] are expected to affect not only the nature of the adstructures but also their corresponding adsorption mechanisms. In addition, given that the local C═C bonding environment of dihalogenated ethylenes (with a CC bond order of 2) is quite similar to that of 1,2-dihalogenated benzenes (with a smaller CC bond order of 1.5), it would be of interest to extend our earlier studies on dihalogenated ethylenes [11,12] to 1,2-dihalogenated benzene (DXB) on the 2×1 surface. The present halogenated benzene series therefore provides an important testing ground for investigating not only halogen substitutional effects, but also the effects of aromaticity on the adsorption and thermal chemistry on Si(1 0 0)2×1. Because fluorine substitution is biologically compatible and widely used in drug delivery systems [30], polymer and liquid crystals [31], the present study may also be of practical interest to various biosensor applications.

2. Experimental and computational details

Details of our experimental setup and procedure have been described elsewhere [10,15]. Briefly, all the experiments were performed in a home-built dual-chamber ultra-high vacuum (UHV) system with a base pressure better than 1×10^{-10} Torr. The sample preparation chamber was equipped with an ion-sputtering gun for sample cleaning, and a four-grid retarding-field optics for both reverse-view low energy electron diffraction (LEED) and Auger electron spectroscopy. The analysis chamber was used to conduct TPD studies by using a differentially pumped 1–300 amu quadrupole mass spectrometer (QMS, VG Quadrupole SXP Elite), and XPS experiments by using an electron spectrometer (VG Scientific CLAM-2, consisting of a hemispherical analyser of 100 mm mean radius and a triple-channeltron detector) and a twin-anode X-ray source (that supplied unmonochromatic AlKα radiation with a photon energy of 1486.6 eV) [10]. For the present TPD experiments, a home-built programmable proportional–integral–differential temperature controller was used to provide linear temperature ramping at an adjustable heating rate, typically

set at 2 K/s [15]. XPS spectra were collected with an acceptance angle of ±4° at normal emission from the silicon sample, and with a constant pass energy of 50 eV giving an effective energy resolution of 1.4 eV full-width-at-half-maximum (for the Si 2p photopeak) [10]. The binding energy scale of the XPS spectra has been calibrated to the Si 2p feature of the bulk at 99.3 eV [32]. Spectral fitting and deconvolution based on residual minimization with Gaussian–Lorentzian lineshapes were performed by using the CasaXPS software. For temperature-dependent XPS measurements, the sample was flash-annealed to the preselected temperature and quenched to RT before collecting the XPS spectra. In the case of 1,2-dichlorobenzene (1,2-DCB), the quantification of the surface Cl content based on the Cl 2p photopeak at 200 eV is often obscured by the ill-defined background contribution arising from the nearby Si 2s feature (at 151 eV). In order to avoid this ambiguity, the Cl 2s photopeak was used instead in all the 1,2-DCB experiments.

A $14 \times 7\ mm^2$ substrate was cut from a single-side-polished p-type B-doped Si(1 0 0) wafer (0.4 mm thick) with a resistivity of 0.0080–0.0095 Ω cm. Details of the sample mounting and preparation procedures have been described in our earlier work [15]. The liquid DXB chemicals: 1,2-difluorobenzene (1,2-DFB, 98% purity), 1,2-DCB (99% purity) and 1,2-dibromobenzene (1,2-DBB, 98% purity) were purchased from Aldrich and thoroughly degassed by repeated freeze–pump–thaw cycles prior to use. The DXB chemicals were exposed to the Si sample by backfilling the preparation chamber to an appropriate pressure (as monitored by an uncalibrated ionization gauge) with a variable precision leak valve. All exposures (in units of Langmuir, $1\ L = 1 \times 10^{-6}$ Torr s) were performed at RT, and a saturation coverage was used unless stated otherwise. For experiments involving a sputtered Si surface, a clean Si(1 0 0)2×1 surface was sputtered at 2 keV beam energy (and 17 mA beam current) for 15 min with the chamber backfilled with Ar at 1×10^{-6} Torr. The lack of long-ranged order of the resulting sputtered surface was confirmed by the absence of LEED spots.

The purities of the DXB chemicals, with the exception of 1,2-DBB, were confirmed by their corresponding cracking patterns obtained in situ in the gas phase by using our mass spectrometer [33]. In the case of 1,2-DBB, its gas-phase cracking pattern obtained in situ by using our QMS revealed a small amount (9%) of benzene. We have made numerous attempts to remove this impurity without success. The purity of the liquid 1,2-DBB sample has also been double-checked ex-situ using a gas-chromatograph mass spectrometer and no benzene was found. While the exact mechanism is unknown, it is conceivable that benzene could be produced by surface reduction of DBB by hydrogen adsorbed on the inside surface of our stainless steel UHV chamber [34]. Despite the presence of this contaminant, the coadsorption of benzene with 1,2-DBB was found to have no apparent effect on the surface chemistry of 1,2-DBB on Si(1 0 0)2×1 (see below).

All the calculations were performed by using methods based on the density functional theory (DFT) at the B3LYP level with the 6-31G(d) basis set in the Gaussian 03 package [35]. Frequency calculations have also been performed for all the optimized structures in order to identify the local minima and the equilibrium structures. To simulate the Si(1 0 0)2×1 surface, a $Si_{15}H_{16}$ cluster with two Si surface dimers was employed. Both geometries of the cluster and the adsorbate were fully relaxed in all the calculations in order to obtain reliable frequency values. The adsorption energy (ΔE) corresponds to the energy difference between the total energy of an optimized adsorption structure and that of the $Si_{15}H_{16}$ cluster and a free DXB molecule (including the respective zero-point vibrational energy corrections). Although we have repeated our calculations using a larger basis set with more polarization and/or diffuse functions [e.g. 6-31++G(d)] and found that they generally give lower total energies, the orderings of the total energies and relative stabilities of the adstructures are found to follow those of the 6-31G(d) level. The use of the simpler basis set in the present calculations therefore would not affect the qualitative conclusions obtained in the present work. Although a multireference wavefunction has been recently suggested to provide a better simulation of the bare silicon surface [36], the physical interpretation of this type of sophisticated wavefunctions is not trivial. It is therefore of interest to use the DFT method, along with a single-configuration wavefunction of a relatively modest Gaussian basis set, to qualitatively identify the plausible adstructures.

3. Results and discussion

3.1. Overview of room-temperature adsorption

Fig. 1 compares the XPS spectra of saturation exposures (50 L) of 1,2-DFB, 1,2-DCB and 1,2-DBB to Si(1 0 0)2×1 at RT to that of benzene. For benzene on Si(1 0 0)2×1, a single C 1s peak at 284.6 eV was observed (Fig. 1a), in good agreement with the synchrotron-radiation photoemission data obtained at 391 eV photon energy by Fink et al. [37]. Benzene has been found to adsorb on the 2×1 surface at RT, producing $\underline{\mathbf{C}}$–H bond in two different $\underline{\mathbf{C}}$ local environments: $\mathrm{C{=}\underline{\mathbf{C}}{<}^{H}_{C}}$ and $\mathrm{{}^{C}_{Si}{>}\underline{\mathbf{C}}{<}^{H}_{C}}$, with no observable chemical shift [37]. In accord with the early work [37], the feature at 284.6 eV (Fig. 1a) could therefore be assigned to C atoms in both of these bonding arrangements. In Fig. 1b, the corresponding C 1s spectrum of 1,2-DFB on Si(1 0 0)2×1 exhibits two features at 284.6 eV (referred as C_1) and 286.7 eV (referred as C_2). In addition to the C_1 1s feature at 284.6 eV corresponding to C–H (and/or C–Si) bonding as observed for benzene (Fig. 1a), the weaker C_2 1s feature at 286.7 eV (Fig. 1b) could therefore be attributed to C–F bonding. The observed intensity ratio between these two features (2.0) is also consistent with the relative moieties of C atoms

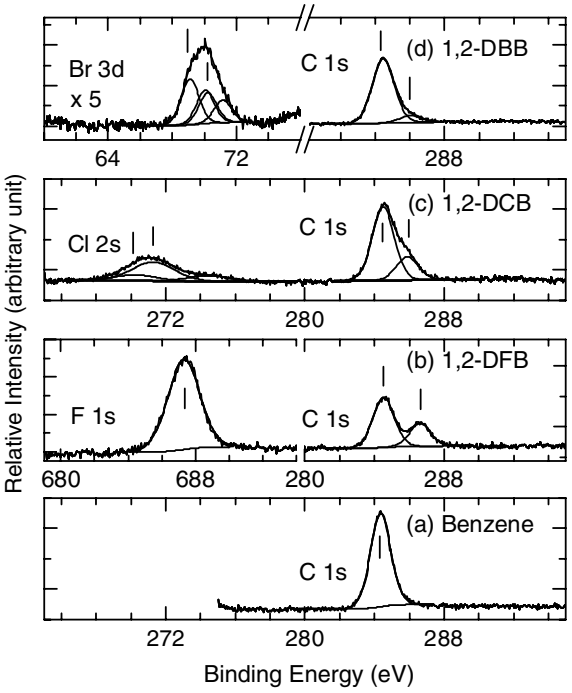

Fig. 1. XPS spectra of 50 L (a) benzene, (b) 1,2-difluorobenzene (1,2-DFB), (c) 1,2-dichlorobenzene (1,2-DCB), and (d) 1,2-dibromobenzene (1,2-DBB) exposed to Si(1 0 0)2 × 1 at room temperature.

bonding to H (4) and F atoms (2). Furthermore, the 2.1 eV shift to higher binding energy found for the C–F feature (with respect to the C–H feature) is in good accord with the strong electron-withdrawing property of F due to the larger difference in electronegativity between F (3.98) and H (2.1) relative to C (2.55, all in the Pauling scale [38]). In the F 1s region (Fig. 1b), the feature at 687.5 eV can be attributed to F atoms in the F–C bond and not in the F–Si bond, which has been found to be located at a lower binding energy (686.5 eV) [39]. 1,2-DFB is therefore found to adsorb molecularly on Si(1 0 0)2 × 1 at RT, without any defluorination.

Fig. 1c shows the XPS spectra of C 1s and Cl 2s regions for 1,2-DCB on Si(1 0 0)2 × 1. As for the case of 1,2-DFB, the C 1s features at 284.6 eV (C_1) and 286.0 eV (C_2) for 1,2-DCB could be assigned similarly to C atoms involving C–H and/or C–Si bonding and C–Cl bonding, respectively [40]. The smaller binding energy difference between the C_2 1s and the C_1 1s features for 1,2-DCB (1.4 eV) than that for 1,2-DFB (2.1 eV) is in accord with the difference in the electronegativity between Cl (3.16) and F (3.98). However, the intensity ratio of the C_1 1s feature (at 284.6 eV) to C_2 1s feature (at 286.0 eV) for 1,2-DCB is found to be 3.0, in marked contrast to the corresponding ratio found for 1,2-DFB (2.0). The larger C_1/C_2 intensity ratio for 1,2-DCE indicates dechlorination in addition to molecular adsorption. In the case of dechlorination, the breakage of C–Cl bond on the Si surface produces C–Si and Cl–Si bonds, the former of which is expected to have a similar C 1s binding energy as the C–H bond given the similar electronegativities for Si (1.8) and H (2.1). Dechlorination therefore causes an increase in the intensity of the C_1 1s feature (at 284.6 eV) and a corresponding decrease in that of the C_2 1s feature (at 286.0 eV). The observed intensity ratio (3.0) indicates 25% of the C–Cl bonds has undergone dissociation upon adsorption on Si(1 0 0)2 × 1, which is in remarkably good agreement with the 23% dissociation observed by Naumkin et al. by using STM [24]. In the Cl 2s region (Fig. 1c), the broad main peak has been deconvoluted into two close-lying features at 271.2 eV [40] and 270.3 eV, which could be assigned to Cl atoms with the Cl–C and Cl–Si bond, respectively. The weaker Cl 2s feature at 274.3 eV could again be attributed to shake-up (many-body) states as discussed in our previous work [11].

Fig. 1d shows the C 1s and Br 3d XPS spectra of 1,2-DBB on Si(1 0 0)2 × 1. The C 1s features at 284.6 eV (C_1) and 285.9 eV (C_2) correspond to C atoms involving C–H (and/or C–Si) bonding and C–Br bonding, respectively, and are similar to the corresponding C 1s features found for 1,2-DCB (Fig. 1c). The similarity in the binding energies of the C_2 1s features for C–Br and C–Cl could be due to similar electronegativities for Br (2.96) and Cl (3.16). The C_1/C_2 intensity ratio of the two C 1s features at 284.6 eV and 285.9 eV for 1,2-DBB is found to be 9.6, which is considerably larger than the corresponding ratios for 1,2-DCB (3.0) and 1,2-DFB (2.0). As with dechlorination for 1,2-DCB, we can make a similar argument that debromination of 1,2-DBB causes an increase in the intensity of the C_1 1s feature at 284.6 eV and a corresponding decrease in that of the C_2 1s feature at 285.9 eV. The observed C_1/C_2 ratio therefore indicates that the majority (76%) of the C–Br bonds has dissociated upon adsorption. In the Br 3d region, two sets of $3d_{5/2}$ and $3d_{3/2}$ features, each with a spin–orbit splitting of 1.0 eV, are found with the $3d_{5/2}$ peaks located at 69.1 eV and 70.1 eV, which correspond respectively to the Si–Br and C–Br bonds [10]. The intensity ratio of the 3d features for Si–Br and C–Br is estimated to be 1.4, which suggests that 67% of the C–Br bonds have undergone dissociation. The small difference between the amounts of dissociation inferred from the C 1s (76%) and Br 3d (67%) spectra suggests that there could be additional C_1 contribution. The extra C_1 intensity could likely come from the coadsorption of a minor amount of benzene contaminant produced in situ by hydrogenation of 1,2-DBB on metal surfaces, as discussed above.

In summary, the propensity for dehalogenation upon adsorption of DXB follows the order: 1,2-DBB (67%) > 1,2-DCB (25%) > 1,2-DFB (0%, i.e. molecular adsorption). Not surprisingly, this trend follows the same ordering of the enthalpy change upon breakage of the C–X bond and the formation of the Si–X bond: 1,2-DBB (21 kcal/mol) > 1,2-DCB (3 kcal/mol) > 1,2-DFB (0 kcal/mol). The bond strengths for C–Br (67 kcal/mol), C–Cl (95 kcal/mol) and C–F (132 kcal/mol) and those for Si–Br (88 kcal/mol), Si–Cl (98 kcal/mol) and Si–F (132 kcal/mol) are obtained from Ref. [29]. Furthermore, the overall intensities of the C 1s features for all three DXB samples and benzene (all relative to the Si 2p features at 99.3 eV)

are found to be remarkably similar to one another (within 10%). Given that the coverage of benzene on Si(100)2 × 1 was reported to be 0.27 by Taguchi et al. [41], i.e. one adsorbate per two Si dimers (or four Si surface atoms), the coverages for the 1,2-DXB adsorbates are therefore estimated to be approximately 0.25, which suggests that dehalogenation upon adsorption has not changed the surface coverage of the adspecies. It should be noted that we have only considered thermodynamic effects in the present work. However, kinetic effects could also play an important role in the differences observed in the degree of dissociation between 1,2-DCB and 1,2-DBB. For example, Naumkin et al. [25] provided DFT calculation to suggest that dissociation is thermodynamically more favourable than molecular adsorption in the case of 1,2-DCB on Si(100)2 × 1. On the other hand, an activation barrier of 0.8 eV was also found for the dissociation of 1,2-DCB on the 2 × 1 surface [25], which therefore suggests that dissociative adsorption is not kinetically favoured relative to molecular adsorption (i.e., without an activation barrier). This competition between thermodynamical and kinetic control could be responsible for the partial dissociation (25%) found for 1,2-DCB and similarly for the 1,2-DBB system as well.

3.2. Thermal desorption and possible dissociative adstructures

Fig. 2a compares the TPD profile of the parent ion (m/z 78) of 50 L benzene on Si(100)2 × 1 with that on a sputtered Si surface. The two desorption features at 460 K (β) and 540 K (γ) were evidently found to be in good accord with the earlier observations for benzene on Si(100)2 × 1 [15,41,42], both in the temperatures of their desorption maxima and their relative intensities. There is a consensus in the literature that the strong desorption feature, β, with a lower desorption temperature corresponds to the desorption of a cyclohexa-2,5-diene-1,4-diyl adspecies, or CHDD for short (Fig. 2b), formed by a [2+4] cycloaddition reaction upon benzene adsorption [15,41–43]. The CHDD adstructure has been commonly referred as the "butterfly" structure in the literature. However, the nature of the much weaker desorption feature, γ, located at the higher desorption temperature remains under debate. Taguchi et al. [41] and Gokhale et al. [42] assigned this feature to adspecies desorbed from defect sites and/or double-layer step edges. This assignment was based on their observation that at saturation coverage the relative concentration of the γ state (17%) corresponds approximately to the defect density (10–25%). On the other hand, Lopinski et al. [44] proposed a more stable 5-cyclohexene-1,2,3,4-tetrayl adstructure, or CHT for short (Fig. 2c), in addition to the CHDD adspecies (Fig. 2b), based on their ab-initio calculations. From the activation barrier for desorption of this so-called double dimer-bridge adstructure, which they approximated by the respective adsorption energy, they further attributed desorption of this adspecies to the γ state [44]. Our DFT/6-31G(d) calculation also reveals two adsorption structures, with the adsorption energy of the CHDD adspecies (−26.2 kcal/mol, Fig. 2b) found to be less negative than that of the CHT adspecies (−38.9 kcal/mol, Fig. 2c), in good accord with the results from Lopinski et al. [44]. In order to further clarify the assignment of the γ state, we perform XPS and TPD experiments on benzene exposed to a sputtered Si surface, which is believed to have more defect sites. The C 1s spectrum for the sputtered sample (not shown) is similar to that found for the 2 × 1 surface (Fig. 1a) but with its overall intensity significantly reduced to 37% of that found on Si(100)2 × 1. The XPS spectrum is therefore not discriminatory in identifying the local C bonding environments, likely due to the similarities in the electronegativities of C and Si as discussed above. Consistent with the reduction in the overall C 1s spectrum for the sputtered sample, the corresponding TPD profile, shown in Fig. 2a, is found to be also significantly weaker than that for the 2 × 1 surface, which suggests that there are more appropriate sites for benzene adsorption on the 2 × 1 surface than the sputtered surface. However, the sputtered sample also exhibits an additional state, α, with the desorption maximum at a lower temperature (380 K) and stronger relative intensity than the β (460 K) and γ states (540 K). In accord with our earlier work [15], the α state found for the sputtered surface could therefore be attributed to adsorption on defect sites, which favours the hypothesis by

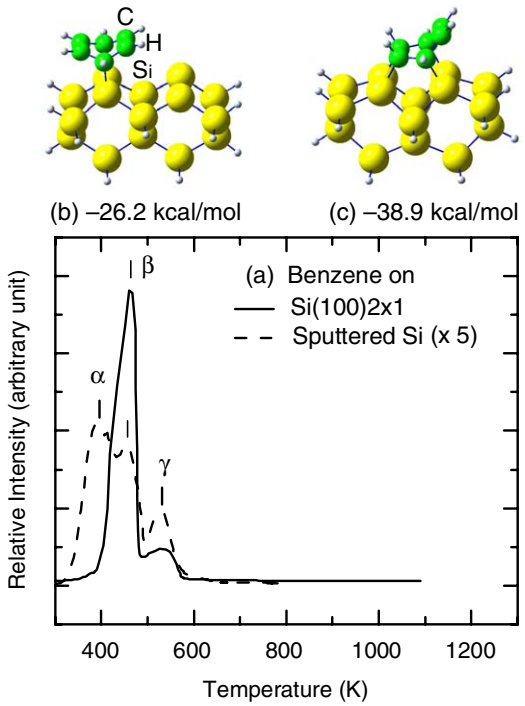

Fig. 2. (a) Temperature programmed desorption profiles of benzene on Si(100)2 × 1, and sputtered Si surface. Equilibrium geometries of plausible adstructures for the (b) β and (c) γ states of benzene on Si(100)2 × 1, obtained by a density functional calculation at the B3LYP/6-31G(d) level with the double-dimer surface of the $Si_{15}H_{16}$ cluster as model for the (2 × 1) surface.

Lopinski et al. [44]. Correspondingly, the γ state, located at the higher temperature, could be assigned to the CHT adstructure (Fig. 2c), in good accord with the more negative adsorption energy. It is noteworthy that in the case of sputtered Si surface, the total C 1s XPS intensities for the adsorption of 1,2-DFB, 1,2-DCB and 1,2-DBB (not shown) are 38%, 82% and 88% of the corresponding intensities found for their adsorption on the 2×1 surface. Evidently, dissociative adsorption (as is evident in the latter two cases) is less surface specific than molecular adsorption, for which the [2+4] cycloaddition requires the existence of appropriate surface dimer sites.

Like benzene on Si(100)2×1, two desorption features of the parent ion (m/z 112) at 450 K and 540 K were found for 1,2-DFB on Si(100)2×1 (Fig. 3b). We also monitored the smaller desorption fragments (e.g., m/z 2, 26, 28, 78) but found no discernible TPD features. The presence of only molecular TPD features is also in good accord with the non-dissociative adsorption inferred from our XPS data shown in Fig. 1b. The similar desorption temperatures found for 1,2-DFB and benzene suggest that the adsorption of 1,2-DFB involves adstructures with similar bonding to those of benzene and that the F atoms in 1,2-DFB appear to be not directly involved in the adsorption. In particular, we could similarly assign the TPD features at 450 K and 540 K, respectively, to the corresponding difluorinated derivatives of the di-σ bonded CHDD and tetra-σ bonded CHT adstructures. These TPD features for 1,2-DFB appear to be generally broader than those of benzene, suggesting the presence of more adsorption states

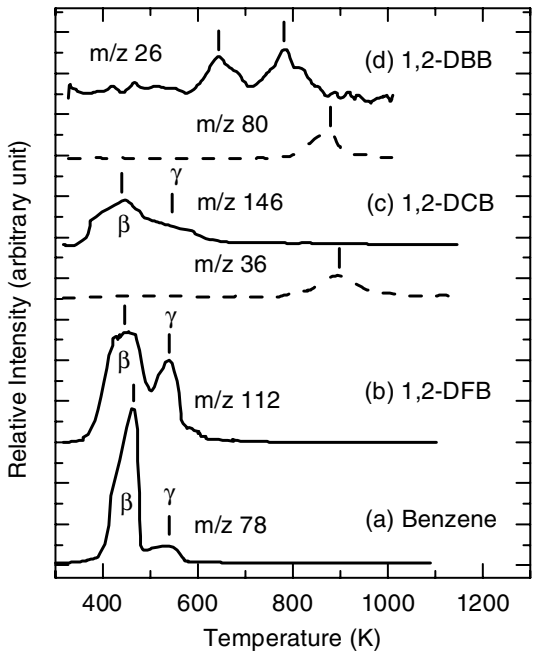

Fig. 3. Temperature programmed desorption profiles of 50 L (a) benzene for m/z 78 ($C_6H_6^+$), (b) 1,2-difluorobenzene (1,2-DFB) for m/z 112 ($C_6H_4F_2^+$), (c) 1,2-dichlorobenzene (1,2-DCB) for m/z 146 ($C_6H_4Cl_2^+$) and m/z 36 (HCl^+), and (d) 1,2-dibromobenzene (1,2-DBB) for m/z 26 ($C_2H_2^+$) and 80 (HBr^+), all exposed to Si(100)2×1 at room temperature.

with similar adsorption energies. It is also of interest to note that the relative intensity of the γ state to that of the β state is considerably larger for 1,2-DFB (Fig. 3b) than that for benzene (Fig. 3a). However, it is generally difficult to infer the relative populations of the adsorption states at RT from the relative intensities of the TPD features [45], beyond the often employed Redhead treatment [46]. In the "static" model of thermal desorption, the enhancement in the relative intensity of the γ state could indicate the presence of more isomer adstructures for the γ state of 1,2-DFB. On the other hand, in a more "dynamical" interpretation of thermal desorption, it is possible that the adstructures of the β state could be thermally converted to those of the γ state during the thermal desorption process. Without a detailed dynamical calculation, the inherent ambiguity associated with the interpretation of TPD features does not allow us to determine the nature of the contributions from these relative intensities [45].

Fig. 3c shows two broad TPD features of the parent ion (m/z 146) for 1,2-DCB on Si(100)2×1. The presence of the molecular desorption features supports our earlier XPS observation of molecular adsorption of 1,2-DCB on Si(100)2×1 (Fig. 1c). Like the 1,2-DFB case, the molecular desorption features at 450 K and near 540 K could be attributed to the dichlorinated derivatives of CHDD and CHT adstructures, respectively. In addition to these two adstructures, Naumkin et al. also observed with STM [24] and proposed a third molecular adstructure for DCB on Si(100)2×1, which involves a CHDD adspecies in between two dimer rows that exhibits a similar adsorption energy as that within a dimer row [25]. However, given that only 8% of the total adspecies was found to correspond to this third adstructure [24], we have not considered this adstructure any further. Of the other ion fragments (m/z 2, 26, 28, 36, 76, and 78) that we also monitored in our TPD experiment for 1,2-DCB, only the TPD profile of m/z 36 reveals any discernible feature. The presence of the m/z 36 feature at 880 K corresponds to recombinative desorption of HCl from dissociated H and Cl atoms on the 2×1 surface, which is consistent with our XPS data (Fig. 1c) that supports partial dechlorination upon RT adsorption of 1,2-DCB. However, we cannot rule out dechlorination of any other Cl-containing adstructures during the thermal desorption process. Given the larger overall m/z 146 TPD intensity than the m/z 36 intensity, most of the molecular adspecies appear to have undergone desorption instead of dechlorination. It is of interest to note that no m/z 2 TPD feature is observed for 1,2-DCB, in contrast to 1,2-dichloroethylene [11]. This result indicates that decomposition of 1,2-DCB to produce H is not a predominant process and HCl desorption provides the main channel for H removal from the surface.

Fig. 3d shows the TPD profiles of m/z 80 and m/z 26, corresponding to the parent ions of HBr^+ and $C_2H_2^+$ respectively, for 1,2-DBB on Si(100)2×1. Other fragments including $C_6H_4Br_2^+$ (m/z 236), Br_2^+ (m/z 160), and H_2^+ (m/z 2) have also been monitored and found to exhibit no TPD

features. In the case of m/z 78 ($C_6H_6^+$ or the parent ion of benzene), a weak desorption profile similar to that of benzene (Fig. 3a) is observed (not shown) and it confirms the coadsorption of benzene produced by reduction (as discussed earlier). In marked contrast to 1,2-DFB and 1,2-DCB, no molecular desorption feature (m/z 236) is observed for 1,2-DBB on the 2×1 surface. Furthermore, our XPS result (Fig. 1d) shows that 76% of the C–Br bonds have been broken upon adsorption, which therefore suggests that 48% of the adspecies have undergone single-debromination, with the rest undergone double-debromination. The $C_2H_2^+$ (m/z 26) features at 640 K and 780 K (Fig. 3d) could be attributed to further decomposition products arising from the bromophenyl ($C_6H_4Br\cdot$) and phenylene (C_6H_4:) debrominated adspecies. Like 1,2-DCB, recombinative desorption of HX (HBr, m/z 80) for 1,2-DBB is also found to occur at 870 K. The similarity in the recombinative desorption temperature for both 1,2-DCB and 1,2-DBB suggests a similar desorption mechanism.

The similar molecular desorption features for 1,2-DFB and 1,2-DCB to that of benzene obtained in the TPD experiments are consistent with the XPS results, which show that the RT adsorption of 1,2-DFB and 1,2-DCB on Si(100)2×1 occurs predominantly via the benzene ring. Following the assignment for the desorption features of benzene on Si(100)2×1, these two molecular desorption states near 460 K and 540 K can be attributed to di-σ bonded dihalo-CHDD isomeric adstructures and tetra-σ bonded dihalo-CHT isomeric adstructures, respectively. These isomeric molecular adstructures (not shown) arising from the double halogen substitution of CHDD (Fig. 2b) and CHT adstructures (Fig. 2c) have been determined by DFT/6-31G(d) calculations. In particular, the two possible dihalo-CHDD isomer adstructures, with similar adsorption energies (−23.5 kcal/mol and −24.0 kcal/mol for 1,2-DFB, −22.8 kcal/mol and −27.0 kcal/mol for 1,2-DCB, and −27.6 kcal/mol and −29.5 kcal/mol for 1,2-DBB) are generally less stable (by at least 8 kcal/mol) than the four dihalo-CHT isomer adstructures also with similar adsorption energies to one another (−36.7 to −39.0 kcal/mol for 1,2-DFB, −34.4 to −41.7 kcal/mol for 1,2-DCB, and −42.8 to −46.4 kcal/mol for 1,2-DBB). Fig. 4 shows the possible dissociative adstructures. Following our TPD results (Fig. 3) and in accord with the work of Naumkin et al. [25], we consider only dehalogenated and not dehydrogenated dissociated adstructures. Evidently, the single-dehalogenated (out-of-dimer-plane) halophenyl adstructures (Fig. 4a, d, g) are generally less stable than the two corresponding double-dehalogenated phenylene adstructures (Fig. 4) by at least 47 kcal/mol. Furthermore, the out-of-dimer-plane phenylene adstructures (Fig. 4b, e, h) are more stable than the corresponding in-dimer-plane adstructures (Fig. 4c, f, i) by at least 10 kcal/mol. These dehalogenated adstructures (halophenyl and phenylene) are considerably more stable than the molecular adstructures (dihalo-CHDD and dihalo-CHT) and they could represent the precursors for the smaller dissociated desorption products (including C_2H_2, HCl, and HBr) observed at higher temperatures in our TPD experiments.

The DFT calculations show that the calculated adstructures for all three 1,2-DXB homologs generally exhibit the same ordering in their stabilities, with dihalo-CHDD < dihalo-CHT < halophenyl < phenylene. Based on these calculated thermodynamical data, we would expect all three homologs to have the same adsorption products. However, the XPS and TPD results of 1,2-DBB and 1,2-DFB reveal evidence of predominant dissociated and exclusive molecular desorption products, respectively, while those for 1,2-DCB exhibit both dissociative and molecular adsorption. These differences in the experimental results among the three homologs from the calculations suggest that kinetic effects play an important competing role to the thermodynamical stabilities of the possible adstructures (Fig. 4). Kinetic effects must therefore be considered in future computational studies to better follow the different adsorption pathways among the three 1,2-DXB homologs.

3.3. Temperature-dependent XPS studies

Fig. 5 shows the C 1s and F 1s XPS spectra of 50 L 1,2-DFB exposed to Si(100)2×1 at RT and their evolution upon sequential flash-annealing to 425 K, 560 K, 700 K, 880 K and 1000 K. Upon annealing to 425 K, both the C_1 1s feature at 284.6 eV and $C_2$1s feature at 286.7 eV observed at RT (Fig. 1b or Fig. 5a) and the F 1s feature at 687.5 eV have undergone a 20% reduction in intensity without any binding energy shift. Along with the C_1 1s to C_2 1s intensity ratio remaining effectively constant (at 2), the intensity reduction indicates molecular desorption. Further flash-annealing the sample to 560 K has significantly reduced the overall C 1s and F 1s intensities (to 31% and 22%, respectively, Fig. 5c). The C_2 1s feature at 286.7 eV has totally diminished, leaving behind a broader C_1 1s feature at 284.4 eV. The disappearance of the C_2 1s feature indicates that the F-containing hydrocarbon adspecies have either desorbed or dissociated into hydrocarbon fragments and F atoms. The broadening of the C_1 1s feature suggests that the dissociated adspecies have evolved into hydrocarbon fragments with slightly different local bonding environments. In the F 1s region, the peak at 687.5 eV also appears to diminish with the emergence of a new feature at 686.5 eV at 560 K, which indicates F abstraction involving the breakage of the C–F bonds and the formation of Si–F bonds [39]. Annealing the sample to 700 K has not produced any significant spectral changes in the C 1s and F 1s regions (Fig. 5d). At 880 K, a new C 1s feature has emerged at a lower binding energy of 283.0 eV, characteristic of SiC (Fig. 5e). This SiC feature becomes the only prominent C 1s feature above 1000 K (Fig. 5f), which indicates complete destruction of hydrocarbon fragments and the formation of SiC and/or C clusters on the surface. In the F 1s region, the feature at 686.5 eV corresponding to Si–F appears to shift back to 687.5 eV (C–F) with a reduced intensity at 880 K (Fig. 5e), which continues to

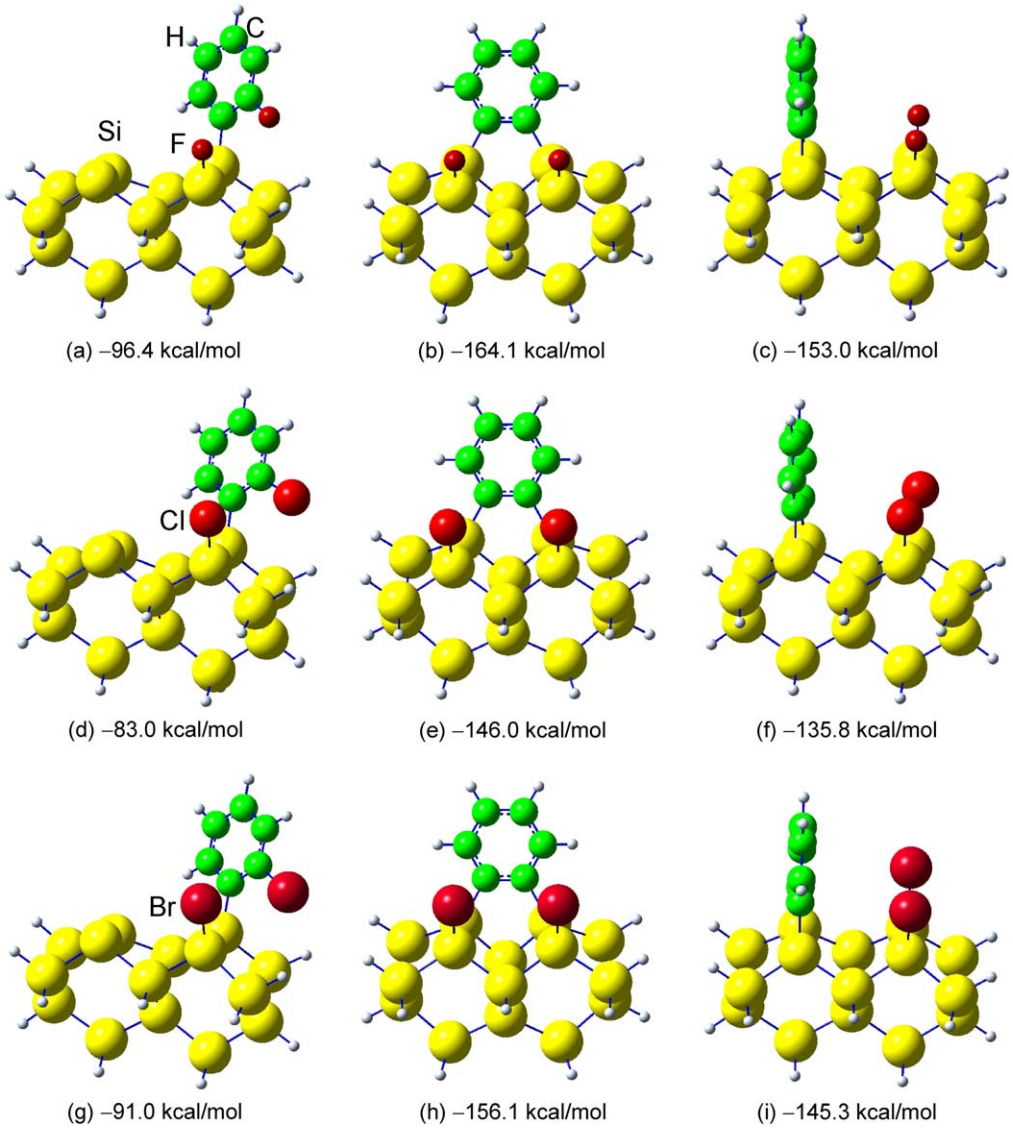

Fig. 4. Equilibrium geometries of plausible dissociative adstructures for 1,2-difluorobenzene (top row), 1,2-dichlorobenzene (middle row) and 1,2-dibromobenzene (bottom row) on a model 2×1 surface of a $Si_{15}H_{16}$ cluster. The dimer row is orientated from left to right direction. The adstructures and their corresponding adsorption energies are obtained by density functional calculations at the B3LYP/6-31G(d) level. The dissociated adstructures include one single-dehalogenated halo-phenyl adstructure (a,d,g) and two double-dehalogenated 1,2-phenylene isomers (b,c,e,f,h,i).

weaken upon further annealing at 1000 K (Fig. 7f). Given the absence of any smaller desorption fragments in our TPD data, the reduction of the F 1s feature above 880 K suggests F diffusion into the bulk.

The spectral evolution of the Cl 2s and C 1s XPS spectra as a function of the flash-annealing temperature for 50 L 1,2-DCB on Si(1 0 0)2×1 is shown in Fig. 6. Flash-annealing to 425 K caused a small general intensity reduction (~10%) for both the C 1s and Cl 2s envelops (Fig. 6b), which is consistent with the molecular desorption observed in the TPD experiments (Fig. 3c). The low-temperature flash-anneal to 425 K of the 1,2-DCB sample, unlike the 1,2-DFB sample, has evidently reduced the C_2 1s component to a greater extent than the C_1 1s component, causing the C_1/C_2 intensity ratio to increase to 4.3. Because the C_2 1s feature (at 286.0 eV) corresponds to the C–Cl bond while the C_1 1s feature (at 284.6 eV) is attributed to the C–H and/or C–Si bonds, the increasing C_1/C_2 intensity ratio indicates Cl abstraction. Further annealing the 1,2-DCB sample to 560 K caused further intensity reduction by 25% in the overall Cl 2s and C 1s spectra (Fig. 6c), again indicative of molecular desorption. The corresponding C_1/C_2 intensity ratio also increases to 10 and the Cl 2s feature undergoes a discernible shift from 271.2 eV (corresponding to Cl–C) to 270.3 eV (corresponding to Cl–Si), both of which indicate further Cl abstraction. (It should be noted that the small feature at 274.3 eV has been assigned to a Cl 2s shake-up peak, as discussed in our earlier work [11].) At 700 K, the C_2 1s component has disappeared completely while no further shift in the Cl 2s feature at 270.3 eV

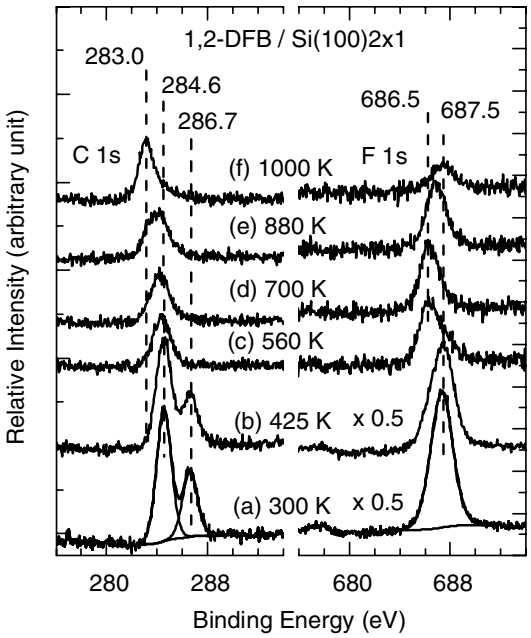

Fig. 5. XPS spectra of the C 1s and F 1s regions of 50 L 1,2-difluorobenzene (1,2-DFB) exposed to Si(100)2 × 1 at (a) 300 K, and upon sequential flash-annealing to (b) 425 K, (c) 560 K, (d) 700 K, (e) 880 K and (f) 1000 K.

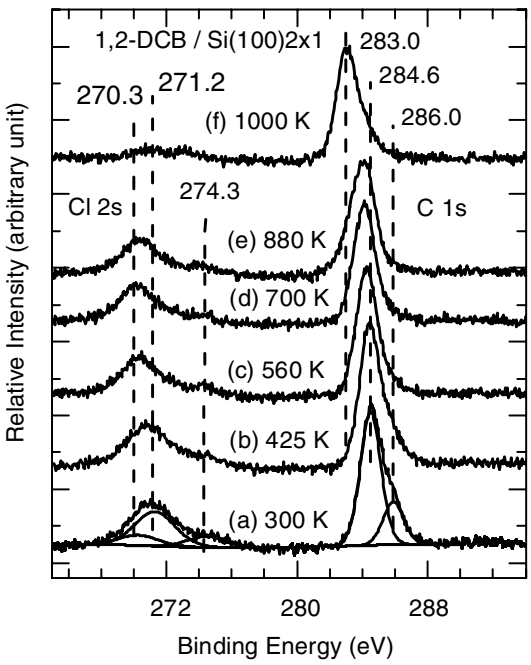

Fig. 6. XPS spectra of the C 1s and Cl 2s regions of 50 L 1,2-dichlorobenzene (1,2-DCB) exposed to Si(100)2 × 1 at (a) 300 K, and upon sequential flash-annealing to (b) 425 K, (c) 560 K, (d) 700 K, (e) 880 K and (f) 1000 K.

is observed (Fig. 6d). The corresponding overall Cl 2s and C 1s intensities appear to remain unchanged, which indicates conversion of the C_2 to C_1 component without further desorption of C-containing adspecies and of the abstracted Cl atoms at this temperature. In accord with our TPD data (Fig. 3c), the lack of spectral changes at the flash-annealing temperature of 700 K marks the completion of molecular desorption. From 700 K to 1000 K, the C 1s peak migrates from 284.6 eV to 283.0 eV, characteristic of SiC, with a discernible shoulder near 284.4 eV that is indicative of C clusters [47]. Complete disappearance of the Cl 2s feature is also observed at a flash-annealing temperature of 1000 K, which is consistent with the removal of Cl through recombinative HCl desorption found in our TPD experiments (Fig. 3c), although we cannot rule out the possibility of Cl diffusion into the bulk at this high annealing temperature.

Fig. 7 shows the Br 3d and C 1s XPS spectra of 50 L 1,2-DBB exposed to Si(100)2 × 1 at RT, and their spectral evolution with increasing flash-annealing temperature. Upon flash-annealing to 425 K (Fig. 7b) and to 560 K (Fig. 7c), a minor but discernible intensity reduction (by 15%) in the strong C_1 1s feature at 284.6 eV (corresponding to the C–H and/or C–Si bond) and the weak C_2 1s feature at 285.9 eV (corresponding to the C–Br bond) are observed (Fig. 7b). The general reduction in the C 1s profile closely follows that found for benzene, which is consistent with the coadsorption of benzene with our 1,2-DBB sample as discussed earlier. Further annealing the sample to 700 K (Fig. 7d) totally eliminates the C_2 1s intensity. The C_1 1s feature remains at the same binding energy location except for a general intensity reduction upon annealing to 700 K and 880 K (Fig. 7e). As with the other samples, annealing to 1000 K (Fig. 7f) generates SiC and C clusters on the surface without any further overall C 1s intensity change. In the Br 3d region, the intensity ratio for Si–Br to C–Br

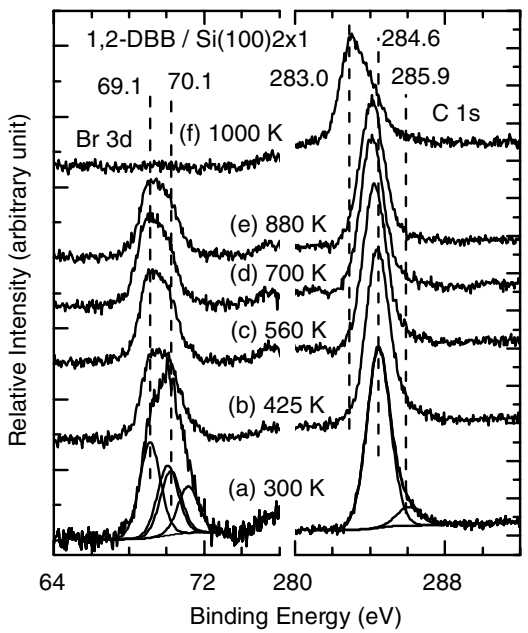

Fig. 7. XPS spectra of the C 1s and Br 3d regions of 50 L 1,2-dibromobenzene (1,2-DBB) exposed to Si(100)2 × 1 at (a) 300 K, and upon sequential flash-annealing to (b) 425 K, (c) 560 K, (d) 700 K, (e) 880 K and (f) 1000 K.

has been shown to be 1.4 at RT (Fig. 7a). The 3d feature for C–Br at 70.1 eV (and 71.2 eV) has evidently been reduced upon annealing to 425 K and has almost completely disappeared at 560 K. On the other hand, the 3d feature for Si–Br at 69.1 eV (and 70.2 eV) has strengthened correspondingly upon annealing to 560 K (Fig. 7c), which suggests further Br abstraction. Furthermore, no decrease in the overall intensity for the 3d band is found below 700 K (Fig. 7d), which is consistent with the TPD data that indicates no molecular desorption (Fig. 3d). Flash-annealing the sample to 880 K causes a 20% intensity reduction in the Br features (Fig. 7e), which completely disappear upon further annealing to 1000 K (Fig. 7f). The observed intensity reduction is in good accord with the on-set of recombinative HBr desorption at 880 K as observed in our TPD experiment. The observed temperature evolution of the C 1s and Br 3d spectra is therefore in good agreement with our TPD data, which show, respectively, the desorption of decomposed hydrocarbon species (C_2H_2) below 800 K and HBr desorption as the only Br removal channel near 880 K.

To summarize the evolution of the 1,2-DXB adstructures remaining on the surface upon sequential flash-annealing, we show in Fig. 8 the intensities (peak areas) of the deconvoluted C 1s and halogen-related XPS features (F 1s for 1,2-DFB, Cl 2s for 1,2-DCB and Br $3d_{5/2}$ for 1,2-DBB), all relative to the Si 2p feature at 99.3 eV, as a function of the annealing temperature. Both the C_1 1s and C_2 1s features corresponding respectively to the C–H and/or C–Si bond and to the C–X bond are illustrated, while the X features for the X–Si and X–C bonds are shown as X_{Si} and X_C respectively in Fig. 8. In general, the adstructures of all three 1,2-DXB exhibit similar thermal evolution pathways. In particular, the general reduction for C_1 1s and C_2 1s from RT to 550 K corresponds to molecular desorption for 1,2-DFB (Fig. 8a) and 1,2-DCB (Fig. 8b). In the case of 1,2-DBB for which our TPD experiment has revealed no parent ion, i.e. no molecular desorbate, the observed C_1 1s reduction is attributed to the desorption of co-adsorbed benzene produced during the exposure of 1,2-DBB, as discussed earlier. As benzene would be completely desorbed by 500 K (Fig. 1a), the presence of benzene as a coadsorbate (less than 10%) is not expected to affect the thermal chemistry of 1,2-DBB. The lack of molecular desorption for 1,2-DBB is also evident from the essentially unchanged temperature profile of the total Br $3d_{5/2}$ intensity (sum of both Br–Si and Br–C features) over this temperature range (Fig. 8c), in contrast to the reduction in the F 1s (Fig. 8a) and Cl 2s (Fig. 8b) found for 1,2-DFB and 1,2-DCB, respectively. In the temperature range 550–700 K, the C_2 1s features, along with the corresponding halogen-related features, have essentially disappeared for all three 1,2-DXB compounds, indicating total destruction of the C–X components in the remaining adspecies. The adspecies for all three DXB therefore generally undergo decomposition and halogen abstraction in this temperature range. Above 700 K (and up to 1000 K), the increase in the C 1s intensity for SiC along with the concomitant weakening of the C_1 1s feature is observed for all three DXB, which indicates further decomposition of the remaining hydrocarbon adspecies into SiC and C clusters. Minor intensity reduction is observed for halogen-related features for the X–Si features from 700 K to 880 K, above which these features appear to be totally removed (at 1000 K). This reduction is consistent with the recombinative desorption of hydrogen halide for 1,2-DCB (Fig. 3c) and 1,2-DBB (Fig. 3d) and with the diffusion of F atoms into the bulk in the case of 1,2-DFB (Fig. 3b), as observed in our TPD experiments.

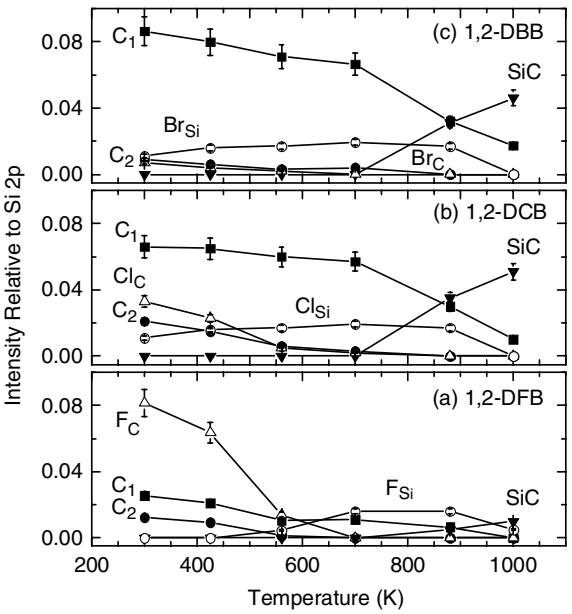

Fig. 8. Spectral intensities of various C 1s and halogen features for 50 L of (a) 1,2-difluorobenzene (1,2-DFB), (b) 1,2-dichlorobenzene (1,2-DCB), and (c) 1,2-dibromobenzene (1,2-DBB) exposed to Si(100)2 × 1 at room temperature, and as a function of the flashing-annealing temperature, all relative to the spectral intensity of the Si 2p feature at 99.3 eV. The C 1s features include C_1 1s (■), C_2 1s (●), and SiC (▼), while the halogen features (F 1s, Cl 2s and Br $3d_{5/2}$) include X_C (△) and X_{Si} (○), corresponding to the respective halogen features of the X–C and X–Si bonds.

The present temperature-dependent XPS data therefore provides a more detailed picture of the thermal evolution of different bonding components of the adspecies remaining on the surface. In the case of 1,2-DXB, the temperature profile of C_2 1s indicates that halogen abstraction occurs below 700 K, discernibly lower than the HX recombinative desorption temperature near 880 K observed in the TPD experiments. From the C 1s profile, molecular desorption is found to be a minor process for 1,2-DCB, which could not be inferred from the relative intensity changes of the TPD profiles. The formation of SiC and C clusters at the higher annealing temperature can only be verified by the present XPS data. The considerably larger relative surface concentrations of SiC and C clusters found for 1,2-DCB and 1,2-DBB than that for 1,2-DFB confirms that molecular desorption predominates in the case of 1,2-DFB.

4. Summary

The RT adsorption and thermal evolution of 1,2-DFB, 1,2-DCB and 1,2-DBB on Si(100)2 × 1 have been examined by TPD and XPS. A transition from predominant molecular adsorption to dissociative adsorption is observed from 1,2-DFB and 1,2-DCB to 1,2-DBB. In particular, the XPS intensity ratio for the C_1 1s to C_2 1s feature is found to be 2 for 1,2-DFB (Fig. 1b), indicating that the adsorption could only follow molecular adsorption without F abstraction. The XPS result is in good accord with the observation of only molecular desorbates in the corresponding TPD profile. In comparison, the C_1/C_2 intensity ratio for 1,2-DCB is found to be 3, which indicates that 25% of the C–Cl bonds has undergone dissociation upon adsorption, supporting the emergence of considerable dissociative adsorption in addition to molecular adsorption. The spectral changes in both C 1s and Cl 2s regions along with the recombinative HCl desorption observed in the TPD experiments show that single and double dechlorination are the primarily dissociative adsorption channels. Finally, dissociative adsorption (i.e., via debromination) is the predominant process for 1,2-DBB on Si(100)2 × 1, as evidenced by the remarkably larger C_1/C_2 XPS intensity ratio (9.6) and the lack of molecular desorbates found in the TPD experiment.

Using DFT calculations at the B3LYP/6-31G(d) level, we propose plausible RT adstructures for 1,2-DXB on the Si(100)2 × 1 surface. In particular, two types of molecular adstructures, including dihalo-CHDD (two isomers) and dihalo-CHT (four isomers), are found. These molecular adstructures could account for the TPD features observed for 1,2-DFB (Fig. 3b) and 1,2-DCB (Fig. 3c), in analogy to those found for benzene on Si(100)2 × 1 (Fig. 3a). Furthermore, halogen abstraction could lead to single-dehalogenated halophenyl (one isomer) and double-dehalogenated 1,2-phenylene (two isomers) adstructures, as illustrated in the DFT calculations (Fig. 4). Thermal evolution of these dehalogenated adstructures could produce the observed TPD products, including HCl for 1,2-DCB (at 900 K), HBr (near 880 K) and C_2H_2 (at 640 K and 780 K) for 1,2-DBB. It is noteworthy that all the isomeric adstructures have similar adsorption energies and as such the present calculations cannot be used to identify the preferred isomer adstructures. Furthermore, the calculated dissociated products show that the benzene ring remains intact, which provides the possibility of using the DXB derivatives to extend the delocalized electron properties in the direction perpendicular to the 2 × 1 surface.

Our DFT calculations also show that the calculated adstructures for all three 1,2-DXB homologs generally exhibit the same ordering in their stabilities, with dihalo-CHDD < dihalo-CHT < halophenyl < phenylene. All three homologs are therefore expected to lead to the same adsorption products. However, the XPS and TPD results of 1,2-DBB and 1,2-DFB reveal evidence of predominant dissociated and exclusive molecular desorption products, respectively, while those for 1,2-DCB show both dissociative and molecular adsorption. These observed differences among the three homologs indicate that kinetic effects play an important competing role to the thermodynamical stabilities of the possible adsorption end-products.

Acknowledgement

This work was supported by the Natural Science and Engineering Research Council of Canada (NSERC).

References

[1] M.C. Hersam, N.P. Guisinger, J.W. Lyding, Nanotechnology 11 (2000) 70.
[2] R.J. Hamers, J.S. Hovis, S. Lee, H. Liu, J. Shan, J. Phys. Chem. B 101 (1997) 1489.
[3] W. Widdra, C. Huang, S.Y. Yi, W.H. Weinberg, J. Chem. Phys. 105 (1996) 5605.
[4] J.S. Hovis, H.B. Liu, R.J. Hamers, J. Phys. Chem. B 102 (1998) 6873.
[5] B. Borovsky, M. Krueger, E. Ganz, Phys. Rev. B 57 (1997) 4269.
[6] N. Witkowski, F. Hennies, A. Pietzsch, S. Mattsson, A. Föhlisch, W. Wurth, M. Nagasono, M.N. Piancastelli, Phys. Rev. B 68 (2003) 115408.
[7] Q. Li, K.T. Leung, Surf. Sci. 541 (2003) 113.
[8] G.T. Wang, C. Mui, J.F. Tannaci, M.A. Filler, C.B. Musgrave, .S.F. Bent, J. Phys. Chem. B 107 (2003) 4982.
[9] M.H. Qiao, F. Tao, Y. Cao, G.Q. Xu, Surf. Sci. 544 (2003) 285.
[10] X.J. Zhou, Q. Li, Z.H. He, X. Yang, K.T. Leung, Surf. Sci. 543 (2003) L668.
[11] X.J. Zhou, Q. Li, K.T. Leung, J. Phys. Chem. B 110 (2006) 5602.
[12] X.J. Zhou, Z.H. He, K.T. Leung, Surf. Sci. 600 (2006) 468.
[13] R.A. Wolkow, Annu. Rev. Phys. Chem. 50 (1999) 413.
[14] P. Kruse, R.A. Wolkow, Appl. Phys. Lett. 81 (2002) 4422.
[15] Q. Li, K.T. Leung, Surf. Sci. 479 (2001) 69.
[16] F. Costanzo, C. Sbraccia, P.L. Silvestrelli, F. Ancilotto, J. Phys. Chem. B 107 (2003) 10209.
[17] S.K. Coulter, J.S. Hovis, M.D. Ellison, R.J. Hamers, J. Vac. Sci. Technol. A 18 (2000) 1965.
[18] Q. Li, Z.H. He, X.J. Zhou, X. Yang, K.T. Leung, Surf. Sci. 560 (2004) 191.
[19] Q. Li, K.T. Leung, J. Phys. Chem. B 109 (2005) 1420.
[20] W.A. Hofer, A.J. Fisher, G.P. Lopinski, R.A. Wolkow, Chem. Phys. Lett. 365 (2002) 129.
[21] M.P. Schwartz, M.D. Ellison, S.K. Coulter, J.S. Hovis, R.J. Hamers, J. Am. Chem. Soc. 122 (2000) 8529.
[22] G.P. Lopinski, D.D.M. Wayner, R.A. Wolkow, Nature 406 (2000) 48.
[23] F. Tao, M.H. Qiao, Z.H. Li, L. Yang, Y.J. Dai, H.G. Huang, G.Q. Xu, Phys. Rev. B 67 (2003) 115334.
[24] F.Y. Naumkin, J.C. Polanyi, D. Rogers, W. Hofer, A. Fisher, Surf. Sci. 547 (2003) 324.
[25] F.Y. Naumkin, J.C. Polanyi, D. Rogers, Surf. Sci. 547 (2003) 335.
[26] P.H. Lu, J.C. Polanyi, D. Rogers, J. Chem. Phys. 112 (2000) 11005.
[27] P.A. Sloan, R.E. Palmer, Nature 434 (2005) 367.
[28] P.Y. Bruice, Organic Chemistry, Prentice-Hall, Upper Saddle River, 1998, p. 623.
[29] D.R. Lide (Ed.), CRC Handbook of Chemistry and Physics, 81st ed., CRC Press, Boca Raton, 2000.
[30] B.K. Park, N.R. Kitteringham, P.M. O'Neill, Annu. Rev. Pharmacol. Toxicol. 41 (2004) 443.
[31] S.J. Tavener, J.H. Clark, J. Fluorine Chem. 123 (2003) 31.
[32] J.F. Moulder, W.F. Stickle, P.E. Sobol, K.D. Bomben, Handbook of X-ray Photoelectron Spectroscopy, Perkin-Elmer, Eden Prairie, 1992.

[33] Mass Spectrometry database, National Institute of Standards and Technology (US), 2005.
[34] V. Bohmer, F. Marschollek, L. Zetta, J. Org. Chem. 52 (1987) 3200.
[35] Gaussian 03 Revision A.1, M.J. Frisch, G.W. Trucks, H.B. Schlegel, G.E. Scuseria, M.A. Robb, J.R. Cheeseman, J.A. Montgomery, Jr., T. Vreven, K.N. Kudin, J.C. Burant, J.M. Millam, S.S. Iyengar, J. Tomasi, V. Barone, B. Mennucci, M. Cossi, G. Scalmani, N. Rega, G.A. Petersson, H. Nakatsuji, M. Hada, M. Ehara, K. Toyota, R.Fukuda, J. Hasegawa, M. Ishida, T. Nakajima, Y. Honda, O. Kitao, H. Nakai, M. Klene, X. Li, J.E. Knox, H.P. Hratchian, J.B. Cross, C. Adamo, J. Jaramillo, R. Gomperts, R.E. Stratmann, O. Yazyev, A.J. Austin, R. Cammi, C. Pomelli, J.W. Ochterski, P.Y. Ayala, K. Morokuma, G.A. Voth, P. Salvador, J.J. Dannenberg, V.G. Zakrzewski, S. Dapprich, A.D. Daniels, M.C. Strain, O. Farkas, D.K. Malick, A.D. Rabuck, K. Raghavachari, J.B. Foresman, J.V. Ortiz, Q. Cui, A.G. Baboul, S. Clifford, J. Cioslowski, B.B. Stefanov, G. Liu, A. Liashenko, P. Piskorz, I. Komaromi, R.L. Martin, D.J. Fox, T. Keith, M.A.Al-Laham, C.Y. Gonzalez, J.A. Pople, Gaussian, Inc., Pittsburgh PA, 2003.
[36] Y. Jung, M.S. Gordon, J. Am. Chem. Soc. 127 (2005) 3131.
[37] A. Fink, W. Widdra, W. Wurth, C. Keller, M. Stichler, A. Achleitner, G. Comelli, S. Lizzit, A. Baraldi, D. Menzel, Phys. Rev. B 64 (2001) 045308.
[38] L. Pauling, The Nature of Chemical Bond, Cornell University Press, Ithaca, 1960.
[39] X. Cao, R.J. Hamers, J. Phys. Chem. B 106 (2002) 1840.
[40] D.T. Clark, D. Kilcast, D.B. Adams, W.K.R. Musgrave, J. Electron Spectrosc. Relat. Phenom. 6 (1975) 117.
[41] Y. Taguchi, M. Fujisawa, T. Takaoka, T. Okada, M. Nishijima, J. Chem. Phys. 95 (1991) 6870.
[42] S. Gokhale, P. Trischberger, D. Menzel, W. Widdra, H. Droge, H.-P. Steinruck, U. Birkenheuer, U. Gutdeutsch, N. Rosch, J. Chem. Phys. 18 (1998) 5554.
[43] M.J. Kong, A.V. Teplyakov, J. Jagmohan, J.G. Lyubovitsky, C. Mui, S.F. Bent, J. Phys. Chem. B 104 (2000) 3000.
[44] G.P. Lopinski, D.J. Moffatt, R.A. Wolkow, Chem. Phys. Lett. 282 (1998) 305.
[45] H. Froitzheim, P. Schenk, G. Wedler, J. Vac. Sci. Technol. A 11 (1993) 345.
[46] P.A. Redhead, Vacuum 48 (1997) 585.
[47] C. Czosnek, J.F. Janik, Z. Olejniczak, J. Cluster Sci. 13 (2002) 487.